Available online at www.sciencedirect.com

ScienceDirect

www.elsevier.com/locate/jes

JES JOURNAL OF ENVIRONMENTAL SCIENCES

www.jesc.ac.cn

Assessing the role of mineral particles in the atmospheric photooxidation of typical carbonyl compound

Yongpeng Ji, Xingyu Chen, Yuqi Xiao, Yuemeng Ji, Weina Zhang, Jiaxin Wang, Jiangyao Chen, Guiying Li, Taicheng An*

Guangdong Key Laboratory of Environmental Catalysis and Health Risk Control, Guangdong-Hong Kong-Macao Joint Laboratory for Contaminants Exposure and Health, Institute of Environmental Health and Pollution control, Key Laboratory of City Cluster Environmental Safety and Green development, School of Environmental Science and Engineering, Guangdong University of Technology, Guangzhou 510006, China

ARTICLE INFO

Article history:
Received 23 October 2020
Revised 21 December 2020
Accepted 21 December 2020
Available online 14 January 2021

Keywords:
Photochemical oxidation
Mineral particles
Acrolein
Reaction mechanism

ABSTRACT

Mineral particles are ubiquitous in the atmosphere and exhibit an important effect on the photooxidation of volatile organic compounds (VOCs). However, the role of mineral particles in the photochemical oxidation mechanism of VOCs remains unclear. Hence, the photooxidation reactions of acrolein (ARL) with OH radical (OH) in the presence and absence of SiO_2 were investigated by theoretical approach. The gas-phase reaction without SiO_2 has two distinct pathways (H-abstraction and OH-addition pathways), and carbonyl-H-abstraction is the dominant pathway. In the presence of SiO_2, the reaction mechanism is changed, i.e., the dominant pathway from carbonyl-H-abstraction to OH-addition to carbonyl C-atom. The energy barrier of OH-addition to carbonyl C-atom deceases 21.33 kcal/mol when SiO_2 is added. Carbonyl H-atom of ARL is occupied by SiO_2 via hydrogen bond, and carbonyl C-atom is activated by SiO_2. Hence, the main product changes from H-abstraction product to OH-adduct in the presence of SiO_2. The OH-adduct exhibits a thermodynamic feasibility to yield HO_2 radical and carboxylic acid via the subsequent reactions with O_2, with implications for O_3 formation and surface acidity of mineral particles.

Introduction

Carbonyl compounds (CCs) are ubiquitous volatile organic compounds (VOCs) in the atmosphere (Dai et al., 2012; Qian et al., 2019; Rao et al., 2016) and are popularly studied for their adverse effects on air quality and human health (Cogliano et al., 2005; Ho et al., 2015; Ji et al., 2013; Tang et al., 2009). They are directly emitted into the atmosphere from the primary anthropogenic and biogenic sources or indirectly emitted as the atmospheric oxidation of other VOCs (Bakeas et al., 2003; Possanzini et al., 2002; Wang et al., 2015; Zheng et al., 2013). Photooxidation of CCs in the gaseous phase plays an important role in the formation of secondary organic aerosols (SOA) and tropospheric ozone (O_3) (Carter, 1994; Clifford et al., 2011; Ji et al., 2018; Mang et al., 2008; Roberts et al., 2001).

Previous studies have revealed that mineral particles exhibit the accommodation properties of VOCs, providing a

* Corresponding author.
E-mail: jiym@gdut.edu.cn (Y. Ji).

https://doi.org/10.1016/j.jes.2020.12.026
1001-0742/

reactive interface for the photooxidation of CCs (Chen et al., 2008; He et al., 2005; Iuga et al., 2010; Ji et al., 2015a, 2015b; Tong et al., 2010; Yao et al., 2017). For example, previous studies have shown that most of mineral particles such as α-Al_2O_3, α-Fe_2O_3, TiO_2 and CaO exhibit good adsorption performance of CCs (Li et al., 2001). That is, CCs irreversibly adsorbed on the surfaces of the above mineral particles. Iuga et al. (2010) have pointed out that the presence of silicate clusters does not change the reaction mechanism of acetaldehyde and OH radical (OH), but affects the contribution of H-abstraction from alkyl chain for the photooxidation reactions of C3-C5 aliphatic aldehydes. Ji et al. (2015b) have revealed that the presence of SiO_2 facilitates the atmospheric reaction of formaldehyde with NO_2. Furthermore, the product yields of ozonolysis for methacrolein and methyl vinyl ketone are larger on SiO_2 surface than that in gas phase (Chen et al., 2008). Considering that mineral particles are a significant class of natural aerosols with the global emissions of 500–4400 Tg/year (Huneeus et al., 2011), therefore, it is essential to study the detailed chemical mechanism of CCs oxidation on the mineral particles and the role of mineral particles in the photooxidation of CCs.

Acrolein (ARL), with both double bond and carbonyl group, is the simplest and typical unsaturated CC with wide emissions from the vehicle exhaust, industrial manufacture, and other sources (Grosjean et al., 2001; Ho and Yu, 2002; Reda et al., 2015; Seaman et al., 2007). By investigating ARL, we can evaluate the impact of the different groups such as double bond and carbonyl group on the reaction mechanism. Although the environmental concentration of ARL is not as high as those of carbonyl compounds such as methylglyoxal and glyoxal, but ARL still can't be neglected in the atmosphere. For example, during the Beijing Olympics, the average concentration of ARL was reported as 2.9 ± 0.8 μg/m^3 (Altemose et al., 2015). The summertime concentrations of ARL range from 75 to 625 ng/m^3 in Roseville, CA (Spada et al., 2008). In the Eastern USA, the median outdoor concentration of ARL is 460 ng/m^3 (Liu et al., 2006). And in Japan, mean outdoor concentration of ARL is 33 ng/m^3 (Azuma et al., 2007). In the coastal regions of southern Europe, the concentration of ARL is comparable to that of acetaldehyde (Romagnoli et al., 2016). During summer in California, USA, the natural background concentration of ARL is higher than 20 ng/m^3 (Cahill, 2014). Furthermore, the photooxidation of ARL forms peroxyacetyl nitrate (PAN)-type species in the presence of NO_x (Magneron et al., 2002; Orlando and Tyndall, 2002). Previous study has shown that the reactive uptake of ARL by aerosols leads to the formation of light-absorbing heterocyclic nitrogen-containing organic compounds in SOA (Li et al., 2019). A recent study showed that the mixing state of mineral dust aerosols with acrolein (ARL) is largely facilitated in the polluted region, with profound implications of the thermodynamic and optical properties of mineral particles (Ji et al., 2019).

Hence, we investigated the photooxidation reactions of ARL in the presence and absence of mineral particles by the first principle theory. Herein, silica (SiO_2), as the largest natural mass of mineral oxidation particles in the earth's crust (de Leeuw et al., 1999), was chosen as the studied mineral particles. The most stable crystalline form of SiO_2, α-quartz, is performed to simulate the case for the presence of mineral particles. The α-quartz (001) is the most stable surface at the ambient condition (de Leeuw et al., 1999; Rignanese et al., 2004, 2000).The geometries and adsorption configurations were constructed and optimized by density functional theory (DFT). The corresponding structural properties were calculated and analyzed by means of charge density difference (CDD) to insight into the nature of photochemical reaction. The photooxidation mechanisms of ARL with OH were elaborated and compared in the presence and absence of SiO_2 to assess the role of mineral particles on atmospheric photooxidation of CCs.

1. Computational methods

1.1. *Calculation details in the presence of SiO_2*

All the calculations of the heterogeneous reaction were performed with the plane-wave level utilizing the Vienna ab initio simulation package (VASP) (Kresse and Furthmüller, 1996a, 1996b) base on the DFT. The Perdew–Burke–Ernzerhof (PBE) (Perdew et al., 1993) within the generalized gradient approximation (GGA) exchange-correlation functional were carried out to investigate the electron interactions. The core electrons were described with the projector augmented wave (PAW) method (PE, 1994). The kinetic cutoff energy was 400 eV in all the calculations, and the convergence criterion of structural optimization was 0.01 eV/Å. A Monkhorst-Pack k-point grid of $4 \times 4 \times 4$ was used to optimize the unit cell of the SiO_2 bulk. The optimized cell parameters are $a = b = 5.023$ Å and $c = 5.511$ Å, which are in good agreement with the experimental data ($a = b = 4.910$ Å, $c = 5.405$ Å) (Levien et al., 1980) and the other theoretical values ($a = b = 5.052$ Å, $c = 5.547$ Å) (Goumans et al., 2007). The hydroxylated (001) surface of SiO_2 was expanded to 2×2 with 12 Si, 28 O and 16 H atoms, which was also constructed and proven effective in our previous work (Ji et al., 2019). For simplicity, the hydroxylated (001) α-quartz is denoted by SiO_2 hereinafter. In order to eliminate the interactions between each slab, the vacuum zone between the slabs was set to approximately 15 Å. The $2 \times 2 \times 1$ Monkhorst-Pack k-point grid was applied to optimize the SiO_2 surface. The van der Waals interactions were considered using the D2 scheme (PBE-D2) (Grimme, 2006) with the explicit R^{-6} terms to DFT (where R is the atomic distance).

The transition states (TSs) of all possible pathways were explored by using the climbing nudged-elastic band method (CL-NEB) (Henkelman et al., 2000) with the convergence criterion of 0.05 eV/Å. Because the potential energy surface (PES) of the heterogeneous reaction is sensitive to the initial state (IS), herein, the most stable adsorption configuration (ARL-SiO_2) for the mixing reaction of ARL and SiO_2 (Ji et al., 2019) was chosen to construct the IS. In this study, the adsorption energy (ΔE_{ads}) was defined as $\Delta E_{ads} = E_{(SiO2\text{-}Adsorbate)} - (E_{SiO2} + E_{Adsorbate})$, where $E_{(SiO2\text{-}Adsorbate)}$ represents the total energy of the adsorption system, and E_{SiO2} and $E_{Adsorbate}$ are the energies of SiO_2 surface and the individual adsorbate, respectively. The energy barrier (ΔE) and the reaction energy (ΔE_r) were obtained from the formulas of $\Delta E = E_{TS} - E_{IS}$ and $\Delta E_r = E_{Products} - E_{IS}$, respectively, where E_{TS}, E_{IS} and $E_{Products}$ represent the energies of the transition states, the initial states and products in the corresponding pathway, respec-

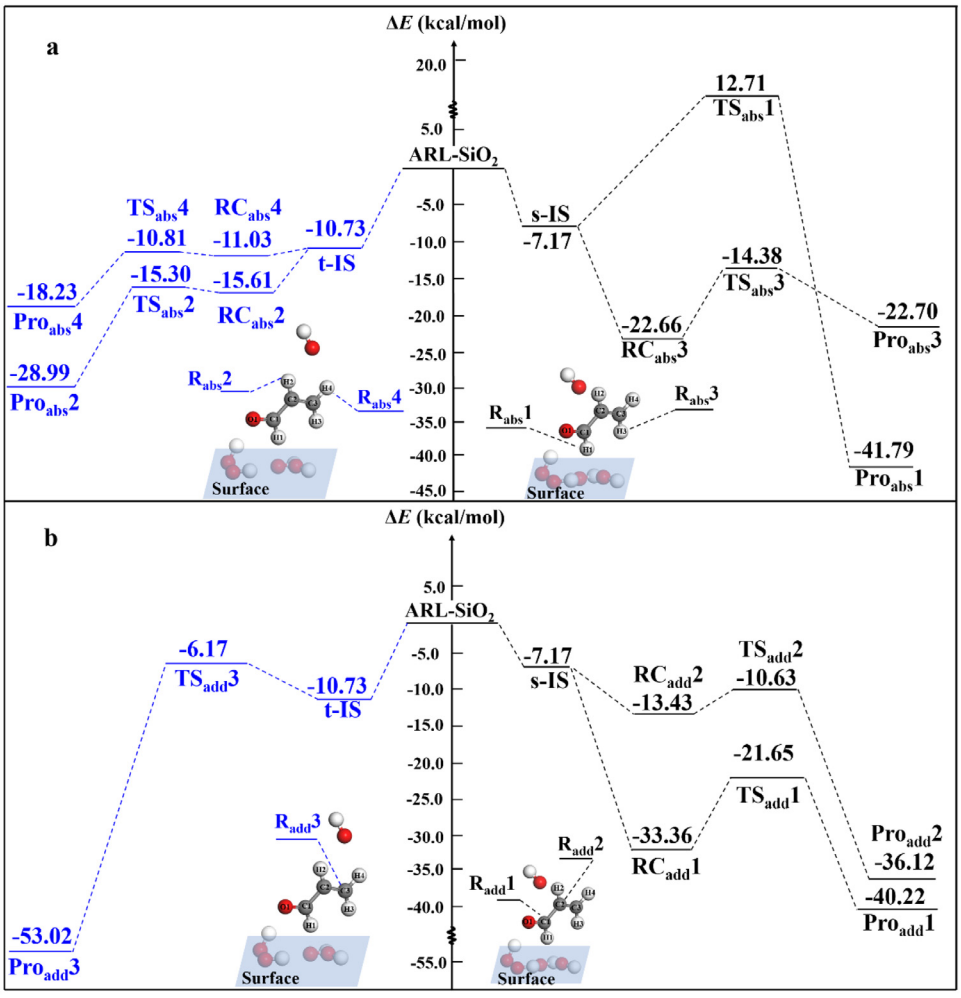

Fig. 1 – Potential energy surfaces of (a) H-abstraction (R_{abs}) and (b) OH-addition (R_{add}) pathways for the photooxidation of acrolein (ARL) on SiO_2 surface. ΔE: the energies relative to the ARL-SiO_2; IS: initial state; RC: pre-reactive complex; TS: transition state; Pro: product.

tively. All the atoms were allowed to be relaxed in all the energy minimization calculations.

1.2. *Calculation details in the absence of SiO_2*

Quantum chemical calculations were performed with Gaussian 09 package (Frisch et al., 2009). Geometry optimization of stationary points, including reactants, complexes, products and TSs, was performed using the density functional M06–2X method (Zhao and Truhlar, 2008) with the 6–311G(d,p) basis set, i.e., the M06–2X/6–311G(d,p) level. The vibrational frequencies were obtained at the same level to identify stationary points to be a local minimum (without any imaginary frequency) or a TS (with only one imaginary frequency). To ascertain that the identified TSs connect the corresponding reactants and products smoothly, the intrinsic reaction coordinate (IRC) calculations were conducted. To yield more accurate energetics, the PES was further refined at the M06–2X/6–311+G(3df,3pd) level on the basis of the above geometries. The dual-level approach, the M06–2X/6–311+G(3df,3pd)//M06–2X/6–311G(d,p) level, was denoted as the M06–2X//M06–2X level. Relative to corresponding reactants, energy barrier ($\Delta E = E_{TS} - E_{Reactants}$) and reaction energy ($\Delta E_r = E_{Products} - E_{Reactants}$) were calculated including zero-point energy (ZPE) corrections.

2. Results and discussion

2.1. *Photooxidation mechanism of ARL with OH on SiO_2 surface*

2.1.1. *Configurations of ISs*

The optimized geometries of ISs are presented in Fig. S1. We chose two local minimums of ISs, in which OH on top and side sites of ARL are denoted as t-IS and s-IS, respectively. The ΔE_{ads} value of t-IS is −10.73 kcal/mol, which is 3.56 kcal/mol lower than that of s-IS (−7.17 kcal/mol), indicating that t-IS is more stable than s-IS. It attributes for two shorter bonds of O_{OH}–H_{ARL} (2.14 and 2.52 Å) in t-IS than those in s-IS (4.05 and 3.51 Å). Two ISs are followed by H-abstraction and OH-addition pathways (Fig. 1). For the H-abstraction pathway, H

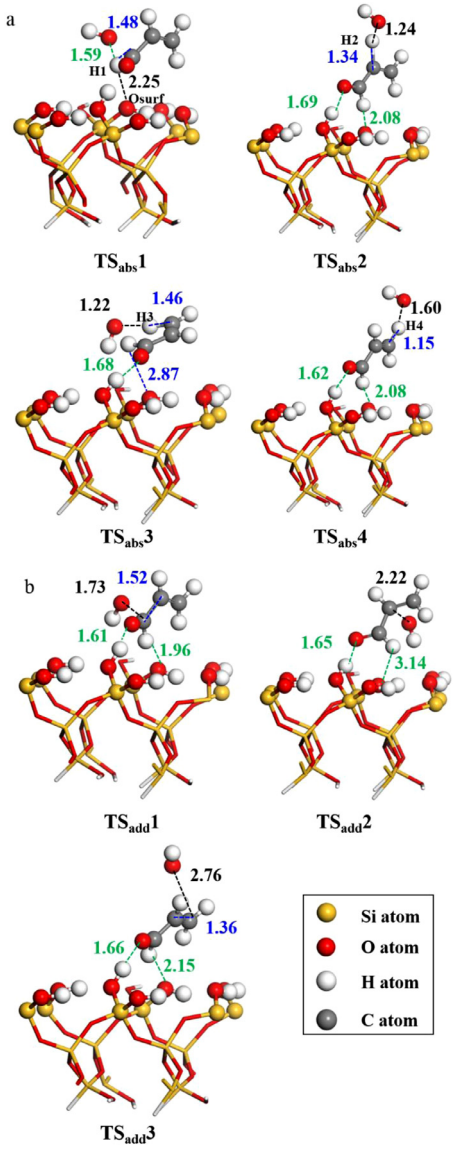

Fig. 2 – Optimized geometries of TSs for (a) H-abstraction and (b) OH-addition pathways in the presence of SiO_2 (unit: Å).

atom is abstracted from carbonyl group ($R_{abs}1$), –CH– ($R_{abs}2$) or $–CH_2–$ ($R_{abs}3/4$) group of ARL. As for the OH-addition pathways, OH adds to carbonyl C-atom ($R_{add}1$) or the middle/terminal methylene C-atom ($R_{add}2/3$). Fig. 1 displays the PESs of all possible pathways for the H-abstraction and OH-addition pathways starting from s-IS and t-IS. The optimized geometries of the stationary points along each pathway are presented in Figs. 2 and S2. The CDD analysis results of key stationary points are displayed in Fig. 3.

2.1.2. *H-abstraction reaction on the SiO_2 surface*

Starting from s-IS (Fig. 1a), there exist two H-abstraction pathways ($R_{abs}1$ and $R_{abs}3$). As shown in Fig. S1, the H-atom (H1) of carbonyl group in s-IS interacts with the surface O-atom (O_{surf}), and the length of H1–O_{surf} bond is 2.10 Å. The CDD analysis of s-IS (Fig. 3a) shows an obvious charge transfer between H1 atom and O_{surf}. It suggests that there is a strong interaction between H1 and O_{surf} atoms, leading to a steric hindrance for H1-abstraction ($R_{abs}1$). For $TS_{abs}1$, the length of H1–O_{surf} bond is increased to 2.25 Å, and the charge transfer of CDD between H1 and O_{surf} weakens in $TS_{abs}1$ (Fig. 3b), indicating the weak interaction between H1 and O_{surf} atoms. Thus, for $R_{abs}1$, the H1-abstraction and the breaking of H1–O_{surf} bond simultaneously occur, leading to the highest ΔE of 19.88 kcal/mol among the four H-abstraction pathways. For $R_{abs}3$, a pre-reactive complex ($RC_{abs}3$) is formed in the entrance of reaction, with the formation energy of −15.49 kcal/mol (Fig. 1a). In $TS_{abs}3$ (Fig. 2a), the length of H3–$C_{methylene}$ bond is 1.46 Å, which is elongated by 0.36 Å relative to $RC_{abs}3$. The ΔE of $R_{abs}3$ pathway is −7.21 kcal/mol, which is 27.09 kcal/mol lower than that of $R_{abs}1$ pathway.

Starting from t-IS, there are also two H-abstraction pathways ($R_{abs}2$ and $R_{abs}4$ pathways). There are complexes $RC_{abs}2$ and $RC_{abs}4$ formed prior to the $TS_{abs}2$ and $TS_{abs}4$ with the stable energies of −4.88 and −0.30 kcal/mol, respectively. As shown in Figs. 2a and S1, the configurations of $TS_{abs}2$ and $TS_{abs}4$ are similar to the configuration of t-IS, indicating that there are few steric hindrances to abstract H2 and H4 atoms of ARL. The ΔE of $R_{abs}2$ pathway with −4.57 kcal/mol is 4.49 kcal/mol lower than that of $R_{abs}4$ pathway, while it is 2.64 kcal/mol higher than that of $R_{abs}3$. Hence, $R_{abs}3$ is the dominant pathway for the H-abstraction reaction of ARL with OH on the SiO_2 surface. However, t-IS is thermodynamically more favorable to form than s-IS due to the lower ΔE_{ads} value, and $R_{abs}2$ pathway starting from t-IS has a negative ΔE of −4.57 kcal/mol. Hence, the contribution of $R_{abs}2$ pathway to the H-abstraction pathway of ARL cannot be neglected.

2.1.3. *OH-addition reaction on the SiO_2 surface*

For $R_{add}1$ and $R_{add}2$ pathways, starting from s-IS, there are two pre-reactive complexes ($RC_{add}1$ and $RC_{add}2$) prior to $TS_{add}1$ and $TS_{add}2$, respectively. The energies of $RC_{add}1$ and $RC_{add}2$ are −26.19 and −6.26 kcal/mol, respectively, which are lower than s-IS. As shown in Figs. 2b and S1, the configuration of $TS_{add}1$ is similar to the corresponding s-IS except for the forming O–C bond. The length of the forming O–C bond decreases from 3.80 Å in s-IS to 1.73 Å in $TS_{add}1$. For $TS_{add}2$, the length of the forming O–C bond with 2.22 Å is 0.49 Å longer than that in $TS_{add}1$. The ΔE values of $R_{add}1$ and $R_{add}2$ are −14.48 and −3.46 kcal/mol (Fig. 1b), respectively. The ΔE of $R_{add}1$ is 11.02 kcal/mol lower than that of $R_{add}2$, attributable for no steric hindrance for OH-addition to carbonyl group. In addition, starting from t-IS, $R_{add}3$ possesses a ΔE values with 4.56 kcal/mol, which is 19.04 kcal/mol higher than that of $R_{add}1$. As discussed above, the order of the ΔE for $R_{add}3$ is $\Delta E(R_{add}1) < \Delta E(R_{add}2) < \Delta E(R_{add}3)$, in line with that of the length of the forming O–C bond in TS (r_{O-C}) with $r_{O-C}(R_{add}1) < r_{O-C}(R_{add}2) < r_{O-C}(R_{add}3)$. Hence, $R_{add}1$ is more favorable than other addition pathways. Compared with the dominant H-abstraction pathway ($R_{abs}3$), OH-addition to carbonyl C-atom ($R_{add}1$) has a lower ΔE and a larger ΔE_r, suggesting that in the presence of SiO_2, the OH-addition to the carbonyl group is of major importance in the atmosphere. Moreover, all the DFT results were calculated using the D3BJ scheme and listed in Table S1. As shown in Table S1, Under the DFT-D2 correction

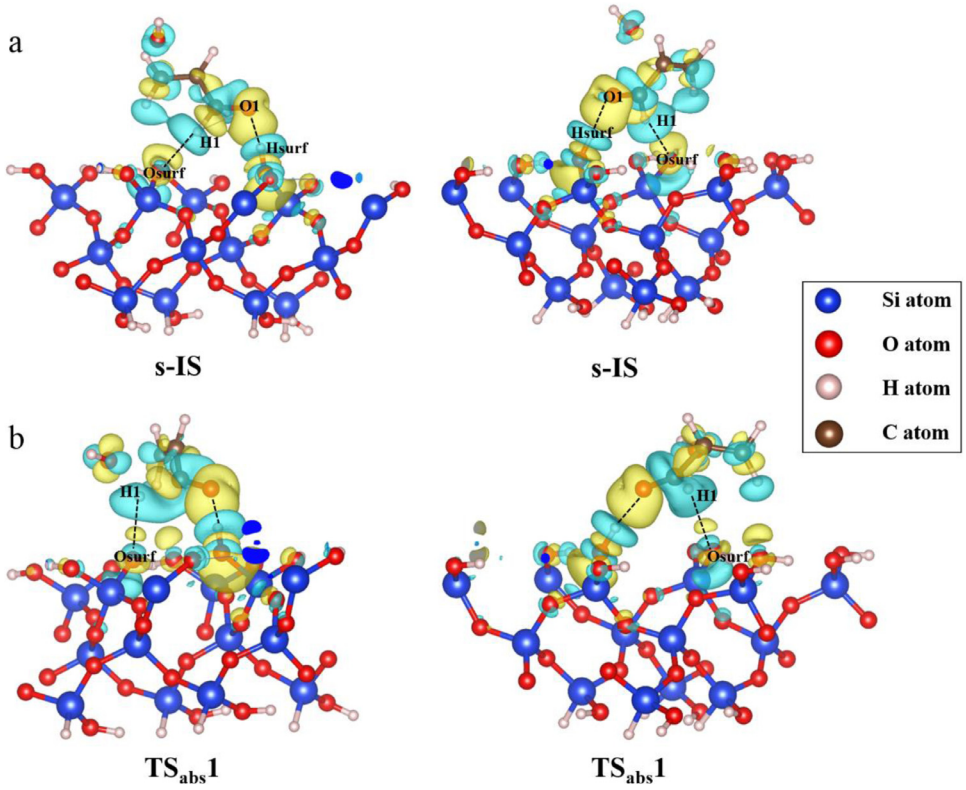

Fig. 3 – Charge density differences of (a) s-IS and (b) $TS_{abs}1$.

method, the order of ΔE for different pathways of ARL is consistent with that of the D3BJ method, suggesting that the DFT results with the D2 scheme is reliable and is suitable for the photooxidation of ARL.

2.2. *Role of SiO_2 in the atmospheric photooxidation of ARL*

To assess the impact of SiO_2 on the atmospheric photooxidation of ARL, we also investigated the photooxidation reaction of ARL and OH without SiO_2. Similar to the reaction system with SiO_2, the reaction also occurs via four H-abstraction and three OH-addition pathways in the absence of SiO_2. For comparison, the nomenclature of the reaction without SiO_2 corresponds to that with SiO_2, except for marking with superscript "gas". The PESs of four H-abstraction and three OH-addition pathways are depicted in Fig. 4. The geometries of all stationary points involved in the gaseous phase reaction are presented in Fig. S3.

For the H-abstraction pathways, the ΔE values of four pathways are −1.85 kcal/mol for $R^{gas}_{abs}1$, 2.24 kcal/mol for $R^{gas}_{abs}2$, 4.73 kcal/mol for $R^{gas}_{abs}3$, and 5.02 kcal/mol for $R^{gas}_{abs}4$ (Fig. 4a). The ΔE of $R^{gas}_{abs}1$ is at least by 4.09 kcal/mol lower than those of other H-abstraction pathways, indicating more favorable carbonyl H_1-abstraction ($R^{gas}_{abs}1$). It is in line with our calculated results of dissociation energy ($D^0_{298}(C-H)$) (Table S2). That is, the $D^0_{298}(C-H)$ in carbonyl group is 88.43 kcal/mol, which is lower than those in other group. However, in the presence of SiO_2, H1 atom on the carbonyl group of ARL is occupied by SiO_2 surface via the formation of hydrogen bond (s-IS in Fig. S1a), causing H1-abstraction pathway undergoes a higher ΔE value and large steric hindrance. In addition, the ΔE values of $R^{gas}_{abs}2$, $R^{gas}_{abs}3$ and $R^{gas}_{abs}4$ are also at least by 5.10 kcal/mol higher than those of the corresponding pathways in the presence of SiO_2. It indicates that the presence of SiO_2 promotes the H-abstraction from the –CH– and $–CH_2–$ groups but hinders the carbonyl-H-abstraction. As discussed above, H-abstraction from the $–CH_2–$ group ($R_{abs}3$) is the dominant H-abstraction pathway on the SiO_2 surface, while H-abstraction from carbonyl group ($R^{gas}_{abs}1$) is the dominant H-abstraction pathway in the absence of SiO_2 surface.

As shown in Fig. 4b, the ΔE values of the three OH-addition pathways are 6.85 kcal/mol for $R^{gas}_{add}1$, 1.03 kcal/mol for $R^{gas}_{add}2$, −0.86 kcal/mol for $R^{gas}_{add}3$. The ΔE corresponds to the order of $R^{gas}_{add}1 > R^{gas}_{add}2 > R^{gas}_{add}3$ in the absence of SiO_2, in contrast to $R_{add}3 > R_{add}2 > R_{add}1$ in the presence of SiO_2. OH-addition to methylene C-atom ($R^{gas}_{add}3$) pathway as the dominant OH-addition pathway becomes difficult to occur when SiO_2 is added, while OH-addition to carbonyl C-atom pathway ($R^{gas}_{add}1$) as the minor OH-addition pathway is of major significance in the presence of SiO_2. It indicates that the carbonyl C-atom is activated.

As discussed above, the ΔE of $R^{gas}_{add}3$ is higher than that of $R^{gas}_{abs}1$, suggesting that H-abstraction from carbonyl group is the most favorable pathway in the absence of SiO_2, in agreement with the previous theoretical results (Olivella and Sole, 2008). Our results suggest that the contribution of OH-addition to carbonyl C-atom is enhanced and becomes a major pathway in the presence of SiO_2. Hence, the presence of SiO_2 changes the photooxidation mechanism of ARL, attributable

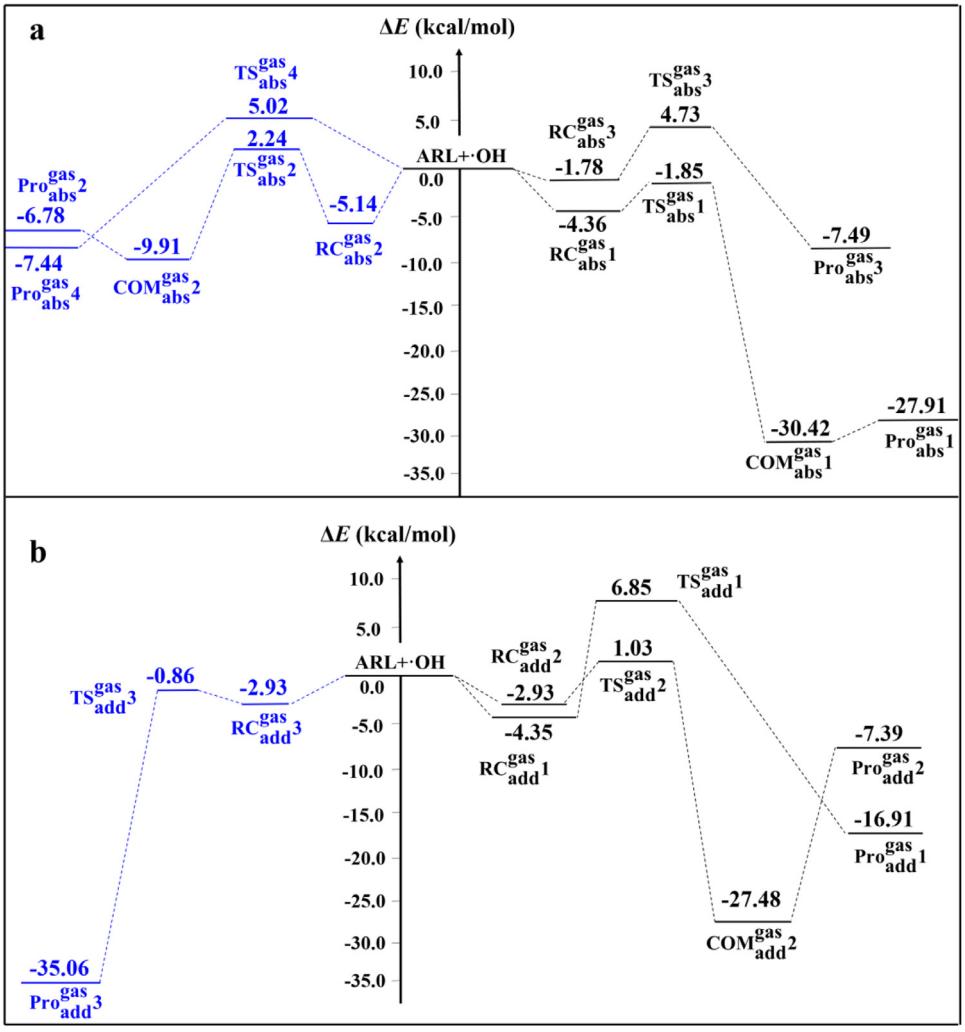

Fig. 4 – Potential energy surfaces of (a) H-abstraction (R^{gas}_{abs}) and (b) OH-addition (R^{gas}_{add}) pathways for the photooxidation of ARL in the absence of SiO_2. COM: the complexes at exit of the reaction.

for the reactivity of carbonyl H-atom and carbonyl C-atom is dominantly affected.

3. Conclusions and atmospheric implications

The photooxidation reaction mechanisms of ARL with OH in the absence and presence of SiO_2 were investigated by DFT. We evaluated the role of mineral particles in the photooxidation of ARL and explored the nature of reaction. In the presence of SiO_2, H-abstraction pathway is of minor importance because carbonyl H-atom is occupied by SiO_2, while OH-addition to carbonyl C-atom is of major significance due to the activated C-atom by SiO_2. Hence, the presence of SiO_2 changes the photooxidation mechanism and product distribution of ARL. For example, for the reaction without SiO_2, the main product is identified to be CH_2CHCO radical, which further reacts with NO_2 and O_2 to form PAN-type species $CH_2CHC(O)O_2NO_2$ (APAN) (Magneron et al., 2002; Orlando and Tyndall, 2002). However, in the presence of SiO_2, the main product changes to RO radical, $CH_2CHCH(OH)O$ radical. Considering that in the troposphere, most of RO radicals have been proven to engage in the reaction with O_2, unimolecular decomposition and unimolecular isomerization (Devolder, 2003; Orlando et al., 2003), we assessed the thermodynamic feasibility of the subsequence reactions of $CH_2CHCH(OH)O$ radical. $CH_2CHCH(OH)O$ radical reacts with O_2 and forms HO_2 radical and $CH_2CHCOOH$, with the ΔE_r of −50.37 kcal/mol, indicating that the reaction is thermodynamic favorable. HO_2 radical further participates in the NO_x chemical cycle and promotes the oxidation of NO to NO_2 and further influences the O_3 formation (Wang et al., 2018). $CH_2CHCOOH$ will be further oxidized by OH through H-abstraction and OH-addition (Chu et al., 2018) or undergoes photodissociation to form OH, CO and CO_2 (Fang and Liu, 2000), which contribute to atmospheric CO_2 and influence the O_3 formation. In addition, $CH_2CHCOOH$ may accumulate on the surface and alter the acidity of SiO_2 surface, and thus influence the acid-catalyzed reactions. However, considering the atmospheric esterification between organic acid and alcohol, it is necessary to investigate whether the acidity of SiO_2 will alter due to the formation of $CH_2CHCOOH$. Moreover, previous studies have

shown that NO_x contributes to the subsequent reaction of the photooxidation products of ARL (Magneron et al., 2002; Orlando and Tyndall, 2002). Hence, the subsequent reaction for the photooxidation products of ARL needed to be further assessed.

In addition, the optimized geometries and the ΔE_{ads} for the adsorption of three gas-phase photooxidation products of ARL on SiO_2 were investigated and the results are list in Appendix A. Supplementary data. As shown in Fig. S5 and Table S3, the most stable adsorption configurations of three products are Pro_a-SiO_2(1), Pro_b-SiO_2(1) and Pro_c-SiO_2(2), with the ΔE_{ads} of −12.38, −18.69 and −8.25 kcal/mol, respectively. It indicates that three gas-phase products are also effectively adsorbed onto SiO_2 surface. Our results revealed that mineral particles not only influence the photooxidation mechanism of CCs but also adsorb the photooxidation products of CCs. Hence, the subsequent conversion of the oxidation products for VOCs in the presence of mineral particles need to be further studied.

Acknowledgments

This work was financially supported by National Natural Science Foundation of China (Nos. 41675122, 42077189 and 41907184), Natural Science Foundation of Guangdong Province, China (No. 2019B151502064), Local Innovative and Research Teams Project of Guangdong Pearl River Talents Program (No. 2017BT01Z032), Innovation Team Project of Guangdong Provincial Department of Education (No. 2017KCXTD012), and Science and Technology Key Project of Guangdong Province, China (No. 2019B110206002).

Appendix A. Supplementary data

Supplementary material associated with this article can be found in the online version at doi:10.1016/j.jes.2020.12.026.

REFERENCES

Altemose, B., Gong, J., Zhu, T., Hu, M., Zhang, L., Cheng, H., et al., 2015. Aldehydes in relation to air pollution sources: a case study around the Beijing Olympics. Atmos. Environ. 109, 61–69.

Azuma, K., Uchiyama, I., Ikeda, K., 2007. The risk screening for indoor air pollution chemicals in Japan. Risk Anal. 27, 1623–1638.

Bakeas, E.B., Argyris, D.I., Siskos, P.A., 2003. Carbonyl compounds in the urban environment of Athens, Greece. Chemosphere 52, 805–813.

Cahill, T.M., 2014. Ambient acrolein concentrations in coastal, remote, and urban regions in California. Environ. Sci. Technol. 48, 8507–8513.

Carter, W.P.L., 1994. Development of ozone reactivity scales for volatile organic compounds. Air Waste 44, 881–899.

Chen, Z.M., Jie, C.Y., Li, S., Wang, H.L., Wang, C.X., Xu, J.R., et al., 2008. Heterogeneous reactions of methacrolein and methyl vinyl ketone: kinetics and mechanisms of uptake and ozonolysis on silicon dioxide. J. Geophys. Res.-Atmos. 113 D22303/22301-D22303/22316.

Chu, H., Wu, W., Shao, Y., Tang, Y., Zhang, Y., Cheng, Y., et al., 2018. A quantum theory investigation on atmospheric oxidation mechanisms of acrylic acid by OH radical and its implication for atmospheric chemistry. Environ. Sci. Pollut. Res. 25, 24939–24950.

Clifford, G.M., Hadj-Aissa, A., Healy, R.M., Mellouki, A., Munoz, A., Wirtz, K., et al., 2011. The atmospheric photolysis of o-tolualdehyde. Environ. Sci. Technol. 45, 9649–9657.

Cogliano, V.J., Grosse, Y., Baan, R.A., Straif, K., Secretan, M.B., El Ghissassi, F., et al., 2005. Meeting report: summary of IARC monographs on formaldehyde, 2-butoxyethanol, and 1-tert-butoxy-2-propanol. Environ. Health Perspect. 113, 1205–1208.

Dai, W.-T., Ho, S.S.H., Ho, K.-F., Cao, J.-J., 2012. Characterization of particulate-phase high molecular weight mono-carbonyls (C# >5) and dicarbonyls in urban atmosphere of Xi'an, China. Aerosol Air Qual. Res. 12, 892–901.

de Leeuw, N.H., Higgins, F.M., Parker, S.C., 1999. Modeling the surface structure and stability of alpha-quartz. J. Phys. Chem. B 103, 1270–1277.

Devolder, P., 2003. Atmospheric fate of small alkoxy radicals: recent experimental and theoretical advances. J. Photoch. Photobio. A 157, 137–147.

Fang, W.H., Liu, R.Z., 2000. Photodissociation of acrylic acid in the gas phase: an ab initio study. J. Am. Chem. Soc. 122, 10886–10894.

Frisch, M.J., Trucks, G.W., Schlegel, H.B., Scuseria, G.E., Robb, M.A., Cheeseman, J.R., et al., 2009. Gaussian 09, Revision D.01. Gaussian, Inc.

Goumans, T.P.M., Wander, A., Brown, W.A., Catlow, C.R.A., 2007. Structure and stability of the (001) alpha-quartz surface. Phys. Chem. Chem. Phys. 9, 2146–2152.

Grimme, S., 2006. Semiempirical GGA-type density functional constructed with a long-range dispersion correction. J. Comput. Chem. 27, 1787–1799.

Grosjean, D., Grosjean, E., Gertler, A.W., 2001. On-road emissions of carbonyls from light-duty and heavy-duty vehicles. Environ. Sci. Technol. 35, 45–53.

He, H., Liu, J., Mu, Y., Yu, Y., Chen, M., 2005. Heterogeneous oxidation of carbonyl sulfide on atmospheric particles and alumina. Environ. Sci. Technol. 39, 9637–9642.

Henkelman, G., Uberuaga, B.P., Jonsson, H., 2000. A climbing image nudged elastic band method for finding saddle points and minimum energy paths. J. Chem. Phys. 113, 9901–9904.

Ho, K.F., Ho, S.S.H., Huang, R.J., Dai, W.T., Cao, J.J., Tian, L., et al., 2015. Spatiotemporal distribution of carbonyl compounds in China. Environ. Pollut. 197, 316–324.

Ho, S.S.H., Yu, J.Z., 2002. Concentrations of formaldehyde and other carbonyls in environments affected by incense burning. J. Environ. Monit. 4, 728–733.

Huneeus, N., Schulz, M., Balkanski, Y., Griesfeller, J., Prospero, J., Kinne, S., et al., 2011. Global dust model intercomparison in AeroCom phase I. Atmos. Chem. Phys. 11, 7781–7816.

Iuga, C., Ignacio Sainz-Diaz, C., Vivier-Bunge, A., 2010. On the OH initiated oxidation of C2-C5 aliphatic aldehydes in the presence of mineral aerosols. Geochim. Cosmochim. Acta 74, 3587–3597.

Ji, Y., Chen, X., Li, Y., Zhang, W., Shi, Q., Chen, J., et al., 2019. The mixing state of mineral dusts with typical anthropogenic pollutants: a mechanism study. Atmos. Environ. 209, 192–200.

Ji, Y., Wang, H., Chen, J., Li, G., An, T., Zhao, X., 2015a. Can silica particles reduce air pollution by facilitating the reactions of aliphatic aldehyde and NO_2? J. Phys. Chem. A 119, 11376–11383.

Ji, Y., Wang, H., Li, G., An, T., 2015b. Theoretical investigation on the role of mineral dust aerosol in atmospheric reaction: a case of the heterogeneous reaction of formaldehyde with NO_2 onto SiO_2 dust surface. Atmos. Environ. 103, 207–214.

Ji, Y., Zheng, J., Qin, D., Li, Y., Gao, Y., Yao, M., et al., 2018. OH-initiated oxidation of acetylacetone: implications for ozone and secondary organic aerosol formation. Environ. Sci. Technol. 52, 11169–11177.
Ji, Y.M., Wang, H.H., Gao, Y.P., Li, G.Y., An, T.C., 2013. A theoretical model on the formation mechanism and kinetics of highly toxic air pollutants from halogenated formaldehydes reacted with halogen atoms. Atmos. Chem. Phys. 13, 11277–11286.
Kresse, G., Furthmüller, J., 1996a. Efficiency of ab-initio total energy calculations for metals and semiconductors using a plane-wave basis set. Comp. Mat. Er. Sci. 6, 15–50.
Kresse, G., Furthmüller, J., 1996b. Efficient iterative schemes for ab initio total-energy calculations using a plane-wave basis set. Phys. Rev. B 54, 11169–11186.
Levien, L., Prewitt, C.T., Weidner, D.J., 1980. Structure and elastic properties of quartz at pressure. Am. Mineral. 65, 920–930.
Li, P., Perreau, K.A., Covington, E., Song, C.H., Carmichael, G.R., Grassian, V.H., 2001. Heterogeneous reactions of volatile organic compounds on oxide particles of the most abundant crustal elements: surface reactions of acetaldehyde, acetone, and propionaldehyde on SiO_2, Al_2O_3, Fe_2O_3, TiO_2, and CaO. J. Geophys. Res. Atmos. 106, 5517–5529.
Li, Z., Nizkorodov, S.A., Chen, H., Lu, X., Yang, X., Chen, J., 2019. Nitrogen-containing secondary organic aerosol formation by acrolein reaction with ammonia/ammonium. Atmos. Chem. Phys. 19, 1343–1356.
Liu, W., Zhang, J., Zhang, L., Turpin, B.J., Welsel, C.P., Morandi, M.T., et al., 2006. Estimating contributions of indoor and outdoor sources to indoor carbonyl concentrations in three urban areas of the United States. Atmos. Environ. 40, 2202–2214.
Magneron, I., Thevenet, R., Mellouki, A., Le Bras, G., Moortgat, G.K., Wirtz, K., 2002. A study of the photolysis and OH-initiated oxidation of acrolein and trans-crotonaldehyde. J. Phys. Chem. A 106, 2526–2537.
Mang, S.A., Henricksen, D.K., Bateman, A.P., Andersen, M.P.S., Blake, D.R., Nizkorodov, S.A., 2008. Contribution of carbonyl photochemistry to aging of atmospheric secondary organic aerosol. J. Phys. Chem. A 112, 8337–8344.
Olivella, S., Sole, A., 2008. Mechanisms for the reactions of hydroxyl radicals with acrolein: a theoretical study. J. Chem. Theory Comput. 4, 941–950.
Orlando, J.J., Tyndall, G.S., 2002. Mechanisms for the reactions of OH with two unsaturated aldehydes: crotonaldehyde and acrolein. J. Phys. Chem. A 106, 12252–12259.
Orlando, J.J., Tyndall, G.S., Wallington, T.J., 2003. The atmospheric chemistry of alkoxy radicals. Chem. Rev. 103, 4657–4689.
PE, B., 1994. Projector augmented-wave method. Phys. Rev. B Condens. Matter. 50, 17953–17979.
Perdew, J.P., Chevary, J.A., Vosko, S.H., Jackson, K.A., Pederson, M.R., Singh, D.J., et al., 1993. Atoms, molecules, solids, and surfaces: applications of the generalized gradient approximation for exchange and correlation. Phys. Rev. B Condens. Matter. 46, 6671–6687.
Possanzini, M., Di Palo, V., Cecinato, A., 2002. Sources and photodecomposition of formaldehyde and acetaldehyde in Rome ambient air. Atmos. Environ. 36, 3195–3201.
Qian, X., Shen, H., Chen, Z., 2019. Characterizing summer and winter carbonyl compounds in Beijing atmosphere. Atmos. Environ. 214, 116845.
Rao, Z., Chen, Z., Liang, H., Huang, L., Huang, D., 2016. Carbonyl compounds over urban Beijing: concentrations on haze and non-haze days and effects on radical chemistry. Atmos. Environ. 124, 207–216.
Reda, A.A., Schnelle-Kreis, J., Orasche, J., Abbaszade, G., Lintelmann, J., Arteaga-Salas, J.M., et al., 2015. Gas phase carbonyl compounds in ship emissions: differences between diesel fuel and heavy fuel oil operation. Atmos. Environ. 112, 369–380.
Rignanese, G.M., Charlier, J.C., Gonze, X., 2004. First-principles molecular-dynamics investigation of the hydration mechanisms of the (0001) alpha-quartz surface. Phys. Chem. Chem. Phys. 6, 1920–1925.
Rignanese, G.M., De Vita, A., Charlier, J.C., Gonze, X., Car, R., 2000. First-principles molecular-dynamics study of the (0001) alpha-quartz surface. Phys. Rev. B 61, 13250–13255.
Roberts, J.M., Stroud, C.A., Jobson, B.T., Trainer, M., Hereid, D., Williams, E., et al., 2001. Application of a sequential reaction model to PANs and aldehyde measurements in two urban areas. Geophys. Res. Lett. 28, 4583–4586.
Romagnoli, P., Balducci, C., Perilli, M., Perreca, E., Cecinato, A., 2016. Particulate PAHs and n-alkanes in the air over Southern and Eastern Mediterranean Sea. Chemosphere 159, 516–525.
Seaman, V.Y., Bennett, D.H., Cahill, T.M., 2007. Origin, occurrence, and source emission rate of acrolein in residential indoor air. Environ. Sci. Technol. 41, 6940–6946.
Spada, N., Fujii, E., Cahill, T.M., 2008. Diurnal cycles of acrolein and other small aldehydes in regions impacted by vehicle emissions. Environ. Sci. Technol. 42, 7084–7090.
Tang, X., Bai, Y., Duong, A., Smith, M.T., Li, L., Zhang, L., 2009. Formaldehyde in China: production, consumption, exposure levels, and health effects. Environ. Int. 35, 1210–1224.
Tong, S.R., Wu, L.Y., Ge, M.F., Wang, W.G., Pu, Z.F., 2010. Heterogeneous chemistry of monocarboxylic acids on alpha-Al_2O_3 at different relative humidities. Atmos. Chem. Phys. 10, 7561–7574.
Wang, M., Chen, W., Shao, M., Lu, S., Zeng, L., Hu, M., 2015. Investigation of carbonyl compound sources at a rural site in the Yangtze River Delta region of China. J. Environ. Sci. 28, 128–136.
Wang, Y., Guo, H., Zou, S., Lyu, X., Ling, Z., Cheng, H., et al., 2018. Surface O_3 photochemistry over the South China Sea: application of a near-explicit chemical mechanism box model. Environ. Pollut. 234, 155–166.
Yao, M., Ji, Y., Wang, H., Ao, Z., Li, G., An, T., 2017. Adsorption mechanisms of typical carbonyl-containing volatile organic compounds on anatase TiO_2 (001) surface: a DFT investigation. J. Phys. Chem. C 121, 13717–13722.
Zhao, Y., Truhlar, D.G., 2008. The M06 suite of density functionals for main group thermochemistry, thermochemical kinetics, noncovalent interactions, excited states, and transition elements: two new functionals and systematic testing of four M06-class functionals and 12 other functionals. Theor. Chem. Acc. 120, 215–241.
Zheng, J., Yu, Y., Mo, Z., Zhang, Z., Wang, X., Yin, S., et al., 2013. Industrial sector-based volatile organic compound (VOC) source profiles measured in manufacturing facilities in the Pearl River Delta, China. Sci. Total Environ. 456-457, 127–136.